Phytochemistry Letters 33 (2019) 39–45

Contents lists available at ScienceDirect

Phytochemistry Letters

journal homepage: www.elsevier.com/locate/phytol

Discovery of cycloartane-*type* triterpene saponins from *Mussaenda glabra*

Vu Kim Thu[a], Nguyen Xuan Bach[d], Luu The Anh[e], Do Thi Trang[c], Nguyen Xuan Nhiem[c,d], Bui Huu Tai[c,d], Phan Van Kiem[c,d], Chau Van Minh[c], SeonJu Park[b], Yohan Seo[b], Wan Namkung[b], Seung Hyun Kim[b,*]

[a] Hanoi University of Mining and Geology, Pho Vien, Duc Thang, Bac Tu Liem, Hanoi, Viet Nam
[b] Yonsei Institute of Pharmaceutical Sciences, College of Pharmacy, Yonsei University, Incheon, 406-840, Republic of Korea
[c] Institute of Marine Biochemistry, Vietnam Academy of Science and Technology (VAST), 18 Hoang Quoc Viet, Cau Giay, Hanoi, Viet Nam
[d] Graduate University of Sciences and Technology, VAST, 18 Hoang Quoc Viet, Cau Giay, Hanoi, Viet Nam
[e] Central Institute for Natural Resources and Environmental Studies, Vietnam National National University, 19 Le Thanh Tong, Hoan Kiem, Hanoi, Viet Nam

ARTICLE INFO

Keywords:
Cycloartane
Mussaglaoside
Mussaenda glabra
ANO1 inhibitory activity

ABSTRACT

Five new cycloartane saponins, mussaglaosides A–E (**1**–**5**) together with five known saponins, mussaendoside O, mussaendoside, G mussaendoside U, mussaendoside P, and mussaendoside Q (**6**–**10**) were isolated from the leaves of *Mussaenda glabra*. Their structures were determined on the basis of extensive spectroscopic methods, including 1D-, 2D-NMR, and MS data. All compounds were evaluated for ANO1 inhibitory activity using calcium-activated chloride channel and YFP expressing HT29 cells. Among the tested compounds, compound **6** strongly inhibited chloride channel activity with IC_{50} value of 22.0 ± 1.7 μM without any cytotoxicity.

1. Introduction

Anoctamin-1 (ANO1), a voltage-sensitive calcium-activated chloride channel, is highly expressed in human cancer cells and the gastrointestinal interstitial cells of Cajal. Interestingly, the ANO1 inhibitor decreases the proliferation of ANO1-overexpressed cell lines. Previous studies have demonstrated that inhibition of ANO1 may provide a new targeting approach for antitumor therapy and for inhibiting excessive smooth muscle contraction as well as diarrhea symptoms (Bill et al., 2014; Hwang et al., 2016). Furthermore, studies have been conducted to discover natural products (Namkung et al., 2010; Seo et al., 2016; Zhang et al., 2017) as novel ANO1 inhibitors due to their property of "metabolite-likeness", being biologically active, and acting as a substrate to deliver materials into intracellular sites of action in transporter systems (Harvey et al., 2015).

Mussaenda is a genus of flowering plants (Rubiaceae) that are an important source of natural medicine, consisting of 200 species over the world including 27 species in Vietnam. *Mussaenda* genus has been used in traditional medicine for the treatment of different ailments such as sore throat and stomach illness (Chi, 1999). Phytochemical studies of the *Mussaenda* species have revealed the presence of saponins, particularly unique *N*-triterpene saponins (Mohamed et al., 2016; Weimin et al., 1996) and iridoids (De et al., 2012; Dinda et al., 2008). In addition, these species have been shown to have anti-inflammatory, antioxidant, and anticancer activities (Astalakshmi and Sundara, 2017). *Mussaenda pubescens* has been used for the treatment of diarrhea (Zhao et al., 1994). This paper reports the isolation, structural elucidation, and ANO1 inhibitory activity of five new and five known triterpenoid saponins from *Mussaenda glabra* Vahl (Fig. 1).

2. Results and discussion

Compound **1** was obtained as an amorphous powder and its molecular formula was determined to be $C_{60}H_{95}O_{23}N$ by HR-ESI-MS at m/z 1220.6189 $[M + Na]^+$ (Calcd. for $[C_{60}H_{95}O_{23}NNa]^+$, 1220.6187) see Supplement material. The ^{1}H-NMR spectrum of **1** (methanol-d_4) showed the signals of three olefin protons at δ_H 6.04 (dd, J = 8.8, 14.8 Hz), 6.46 (dd, J = 10.8, 14.8 Hz), and 7.04 (d, J = 10.8 Hz), two protons of the cyclopropane ring at δ_H 0.37 (br s) and 0.57 (br s); five methyl groups at δ_H 0.88 (s), 0.93 (s), 1.04 (d, J = 6.5 Hz), 1.05 (s), and 1.07, (s) assigning to a cycloartane triterpene-*type* aglycone; four anomeric protons at δ_H 4.41 (d, J = 8.0 Hz), 4.84 (br s), 4.90 (d, J = 7.6 Hz), and 5.23 (br s) suggesting the presence of four sugar units. In addition, two methyl groups at δ_H 0.81 (d, J = 7.6 Hz) and 1.34 (d, J = 6.4 Hz), and one amino-methine proton at δ_H 5.02 (d, 7.2 Hz) were assigned to a 2-amino-3-methyl-4-pentanolide (4-hydroxyisoleucine γ-lactone). The ^{13}C-NMR and DEPT spectra (Table 1) revealed the signals of 60 carbons, including 8 non-protonated carbons, 31 methines, 12

* Corresponding author at: College of Pharmacy, Yonsei Institute of Pharmaceutical Sciences, Yonsei University, Incheon, 21983, Republic of Korea.
E-mail address: kimsh11@yonsei.ac.kr (S.H. Kim).

https://doi.org/10.1016/j.phytol.2019.07.006
Received 30 May 2019; Received in revised form 9 July 2019; Accepted 11 July 2019

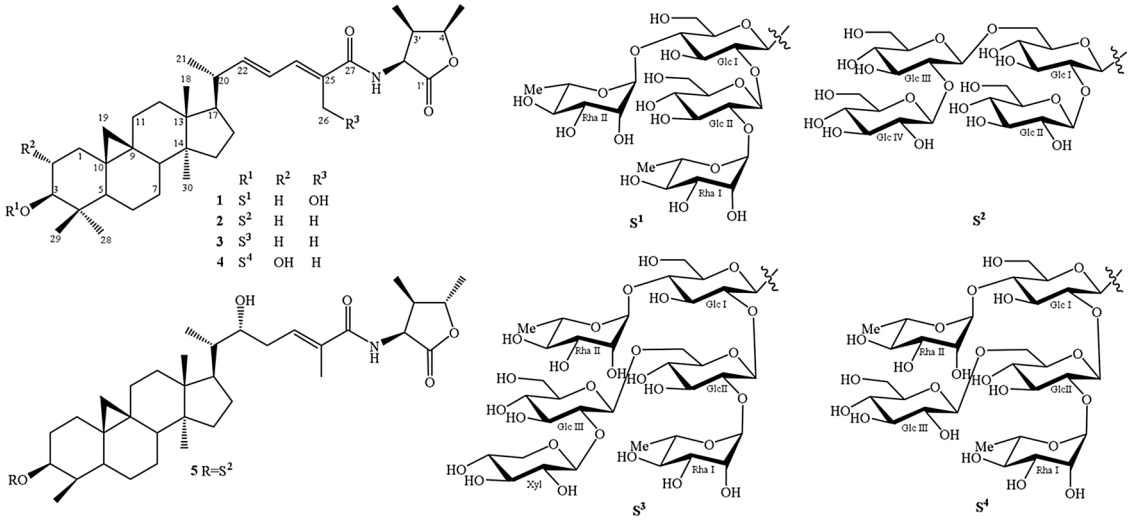

Fig. 1. Chemical structures of compounds **1**–**5**.

methylenes, and 9 methyl carbons. The analysis of ^{1}H- and ^{13}C-NMR data indicated the structure of **1** was similar to that of mussaendoside O (**6**) (Zhao et al., 1994) except for the addition of a hydroxyl group at C-26. The position of this group was proven by HMBC correlations between hydroxymethylene protons H-26 (δ_H 4.43 and 4.47) and C-24 (δ_C 139.5)/C-25 (δ_C 130.6)/C-27 (δ_C 171.1). The HMBC correlations from H_3-21 (δ_H 1.04) to C-17 (δ_C 53.1)/ C-20 (δ_C 42.4)/C-22 (δ_C 152.1); from H-24 (δ_H 7.04) to C-22/C-23 (δ_C 123.6)/C-25 (δ_C 130.6)/C-26 (δ_C 57.4)/C-27 (δ_C 171.1); and from H-22 (δ_H 6.04) to C-17/C-20/C-21 (δ_C 20.1)/C-24 (δ_C 139.5) confirmed the positions of two conjugated double bonds at C-22/C-23 and C-24/C-25 (Fig. 2). The configurations of these double bonds were proven as *E* by the large coupling constant of H-22 and H-23, J = 14.8 Hz, as well as by the NOESY correlations between H-23 (δ_H 6.46) and H_2-26 (δ_H 4.43 and 4.47). The HMBC correlations between hil 3-Me (δ_H 0.81) and hil C-2 (δ_C 56.1)/C-3 (δ_C 39.4)/C-4 (δ_C 78.8), hil 4-Me (δ_H 1.34) and hil C-3/C-4, and the chemical shift of hil H-2 (δ_H 5.02 (d, J = 7.2 Hz)/hil C-2 (δ_C 56.1) and hil H-4 (δ_H 4.74 (m))/C-4 (δ_C 78.8) suggested the presence of a 4-hydroxyisoleucine γ-lactone moiety. The observation of NOESY correlations (Fig. 3) between hil H-2 (δ_H 5.02) and hil H-3 (δ_H 2.83)/hil H-4 (δ_H 4.74); between hil 3-Me (δ_H 0.81) and 4-Me (δ_H 1.34) and the ^{13}C-NMR chemical shift of hil 3-Me (δ_C 8.1) and hil 4-Me (δ_C 15.7) confirmed the configuration of 4-hydroxyisoleucine γ-lactone as [2*S**,3*R**,4*R**] by comparison with those of mussaendoside G [2*S**,3*R**,4*R**] (Weimin et al., 1996) [hil 3-Me (δ_C 8.0) and hil 4-Me (δ_C 15.4)] and (2*S*,3*R*,4*S*)-4-hydroxyisoleucine γ-lactone hydrochloride [3-Me (δ_C 13.0) and 4-Me (δ_C 19.5)] (Wang et al., 2002). 4-hydroxyisoleucine γ-lactone connected with aglycone *via* the amide bond at C-27 was confirmed by HMBC correlations from hil H-2 (δ_H 5.02) and C-27 (δ_C 171.1), a specific amino acid lactone commonly found in the *Mussaenda* genus (Mohamed et al., 2016; Weimin et al., 1996). The HMBC correlations between H_3-28 (δ_H 1.07)/H_3-29 (δ_H 0.88) and C-3 (δ_C 91.5) suggested the position of an oxygenated group at C-3. The α-configuration of H-3 (*axial* orientation) was determined by the observation of NOESY correlations between H-3 (δ_H 3.23) and H-5 (δ_H 1.33)/H_3-28 (δ_H 1.07). Acid hydrolysis of **1** gave L-rhamnose and D-glucose (identified as trimethylsilyl (TMS) derivatives by gas chromatography-mass spectrometry (GC–MS)). In addition, the configurations of sugars in **1**, β-D-glucopyranosyl and α-L-rhamnopyranosyl were supported by the multiplicity of glc I H-1 [δ_H 4.41 (d, J = 8.0 Hz)], glc II H-1 [δ_H 4.90 (d, J = 7.6 Hz)], rha I H-1 [δ_H 5.32 (br s)], and rha II H-1 [δ_H 4.84 (br s)]. The HMBC cross peaks from rha II H-1 (δ_H 4.84) to glc I C-4 (δ_C 79.7), from rha I H-1 (δ_H 5.23) to glc II C-2 (δ_C 78.9), from glc II H-1 (δ_H 4.90) to glc I C-2 (δ_C 78.5), and from glc I H-1 (δ_H 4.41) to C-3 (δ_C 91.5) confirmed the sugar linkages to be α-L-rhamnopyranosyl-(1→2)-*O*-β-D-glucopyranosyl-(1→2)-[α-L-rhamnopyranosyl(1→4)]-*O*-β-D-glucopyranoside and the location of the sugar moiety at C-3 of the aglycone. This sugar moiety has been reported from *Mussaenda pubescens* (Zhao et al., 1994). Consequently, the structure of **1** was determined to be 26-hydroxyheinsiagenin A 3-*O*-α-L-rhamnopyranosyl-(1→2)-*O*-β-D-glucopyranosyl-(1→2)-[α-L-rhamnopyranosyl-(1→4)]-*O*-β-D-glucopyranoside and named mussaglaoside A.

Compound **2** was isolated as an amorphous powder and its molecular formula was determined to be $C_{60}H_{95}O_{24}N$ by HR-ESI-MS at m/z 1236.6134 $[M + Na]^+$ (Calcd. for $[C_{60}H_{95}O_{24}NNa]^+$, 1236.6136). The ^{1}H-NMR spectrum of **2** (methanol-d_4) exhibited the signals of a cycloartane triterpene-*type* aglycone and a 4-hydroxyisoleucine γ-lactone. In addition, four anomeric proton signals at δ_H 5.03 (d, J = 7.2 Hz), 4.65 (d, J = 7.6 Hz), 4.59 (d, J = 7.2 Hz), and 4.37 (d, J = 8.0 Hz) were assigned to four sugar moieties. The ^{13}C-NMR and DEPT spectra of **2** showed the presence of 60 carbons, including 8 non-protonated carbons, 31 methines, 13 methylenes, and 8 methyl carbons. The analytical ^{1}H and ^{13}C NMR spectra of **2** indicated that the aglycone of **2** was similar to heinsiagenin A (Weimin et al., 1996). Acid hydrolysis of **2** gave D-glucose (identified as a TMS derivative). The sugar linkages were determined as β-D-glucopyranosyl-(1→2)-*O*-β-D-glucopyranosyl-(1→6)-[*O*-β-D-glucopyranosyl-(1→2)]-*O*-β-D-glucopyranoside by the observation of HMBC correlations between glc IV H-1 (δ_H 4.59) and glc III C-2 (δ_C 83.2), glc III H-1 (δ_H 5.03) and glc I C-6 (δ_C 69.9), glc II H-1 (δ_H 4.65) and glc I C-2 (δ_C 79.4), and between glc I H-1 (δ_H 4.37) and C-3 (δ_C 91.8) and the location of a sugar at C-3 of the aglycone. Thus, compound **2** was determined as heinsiagenin A 3-*O*-β-D-glucopyranosyl-(1→2)-*O*-β-D-glucopyranosyl-(1→6)-[*O*-β-D-glucopyranosyl-(1→2)]-*O*-β-D-glucopyranoside and named mussaglaoside B.

The molecular formula of **3** was determined as $C_{71}H_{113}O_{31}N$ by the HR-ESI-MS at m/z 1498.7178 $[M + Na]^+$ (Calcd. for $[C_{71}H_{113}O_{31}NNa]^+$, 1498.7189). Similar to those of **2**, the aglycone of **3** was found to be heinsiagenin A (Weimin et al., 1996) by the analytical ^{1}H and ^{13}C NMR data. Acid hydrolysis of **1** confirmed the sugar components as D-glucose, L-rhamnose, and D-xylose. In addition, the multiplicity of six anomeric protons [δ_H 4.34 (d, J = 8.0 Hz, glc I H-1), 4.80 (d, J = 8.0 Hz, glc II H-1), 5.09 (d, J = 7.6 Hz, glc III H-1), 5.20 (br s, rha I H-1), 4.88 (br s, rha II H-1), and 4.52 (d, J = 7.2 Hz, xyl H-1)] suggested the presence of three β-D-glucopyranosyls, two L-rhamnopyranosyls, and one D-xylopyranosyl. Moreover, the HMBC correlations between xyl H-1 (δ_H 4.52) and glc III C-2 (δ_C 83.6), glc III H-1 (δ_H 5.09) and glc II C-6 (δ_C 69.9), rha II H-1 (δ_H 4.88) and glc I C-4 (δ_C 80.1), rha I H-1 (δ_H 5.20) and glc II C-2 (δ_C 79.2), and between glc II H-1 (δ_H 4.80)

Table 1
(Astalakshmi and Sundara, 2017)H- and (Zhang et al., 2017)C-NMR spectroscopic data for compounds **1–5** in CD_3OD.

C	1		2		3		4		5	
	δ_C	δ_H (mult, *J* in Hz)	δ_C	δ_H (mult, *J* in Hz)	δ_C	δ_H (mult, *J* in Hz)	δ_C	δ_H (mult, *J* in Hz)	δ_C	δ_H (mult, *J* in Hz)
Aglycon										
1	33.1	1.27 (m)/1.55 (m)	33.2	1.25 (m)/1.52 (m)	33.2	1.25 (m)/1.50 (m)	40.5	1.46 (m)/1.57 (m)	33.2	1.24 (m)/1.54 (m)
2	30.3	1.73 (m)/2.04 (m)	30.9	1.69 (m)/2.04 (m)	30.9	1.71 (m)/2.03 (m)	70.6	3.75 (m)	30.4	1.72 (m)/2.05 (m)
3	91.5	3.23 (m)	91.8	3.14 (dd, 4.0, 11.6)	92.2	3.12 (dd, 4.0, 12.0)	96.8	2.97 (d, 8.8)	91.8	3.14 (dd, 4.0, 12.0)
4	42.2	–	42.3	–	42.4	–	43.2	–	42.3	–
5	48.4	1.33 (m)	49.0	1.30 (m)	48.4	1.30 (m)	48.7	1.34 (m)	48.4	1.30 (m)
6	22.1	0.80 (m)/1.59 (m	22.2	0.83 (m)/1.63 (m)	22.2	0.83 (m)/1.59 (m)	22.1	0.83 (m)/1.58 (m)	22.2	0.80 (m)/1.59 (m)
7	27.2	1.15 (m)/1.34 (m)	27.2	1.16 (m)/1.31 (m)	27.4	1.15 (m)/1.30 (m)	27.1	1.17 (m)/1.31 (m)	27.4	1.15 (m)/1.32 (m)
8	49.4	1.54 (m)	49.6	1.53 (m)	49.6	1.53 (m)	49.5	1.54 (m)	49.8	1.53 (m)
9	21.1	–	21.1	–	21.1	–	20.4	–	21.2	–
10	27.2	–	27.1	–	27.2	–	26.0	–	27.3	–
11	27.5	1.15 (m)/2.04 (m)	27.4	1.16 (m)/2.02 (m)	27.5	1.16 (m)/2.03 (m)	27.6	1.17 (m)/2.05 (m)	27.5	1.15 (m)/2.02 (m)
12	34.0	1.68 (m)	34.1	1.67 (m)	34.1	1.67 (m)	34.0	1.69 (m)	34.1	1.65 (m)
13	46.7	–	46.7	–	46.8	–	46.7	–	46.9	–
14	50.1	–	50.1	–	50.1	–	50.1	–	49.5	–
15	36.8	1.30 (m)	36.8	1.30 (m)	36.8	1.30 (m)	36.8	1.30 (m)	36.8	1.34 (m)
16	29.4	1.30 (m)/1.74 (m)	29.5	1.30 (m)/1.74 (m)	29.5	1.28 (m)/1.73 (m)	29.5	1.30 (m)/1.74 (m)	28.4	1.37 (m)/1.83 (m)
17	53.1	1.74 (m)	53.2	1.73 (m)	53.2	1.73 (m)	53.1	1.73 (m)	50.5	1.68 (m)
18	19.0	1.05 (s)	18.9	1.05 (s)	18.9	1.05 (s)	19.0	1.05 (s)	18.5	1.02 (s)
19	30.9	0.37 (br s)/0.57 (br s)	30.7	0.36 (br s)/0.57 (br s)	30.9	0.36 (br s)/0.57 (br s)	30.8	0.47 (br s)/0.62 (br s)	30.9	0.35 (s)/0.56 (s)
20	42.4	2.28 (m)	42.5	2.27 (m)	42.5	2.26 (m)	42.2	2.26 (m)	43.9	1.73 (m)
21	20.1	1.04 (d, 6.5)	20.2	1.03 (d, 6.5)	20.2	1.03 (d, 6.5)	20.2	1.04 (d, 6.4)	12.5	0.93 (d, 6.8)
22	152.1	6.04 (dd, 8.8, 14.8)	149.7	5.92 (dd, 8.8, 14.8)	149.7	5.92 (dd, 8.8, 14.8)	149.6	5.93 (dd, 8.8, 14.8)	74.2	3.77 (m)
23	123.6	6.46 (dd, 10.8, 14.8)	124.5	6.34 (dd, 10.8, 14.8)	124.5	6.34 (dd, 10.8, 14.8)	124.6	6.34 (dd, 10.8, 14.8)	30.4	2.16 (m)/2.28 (m)
24	139.5	7.04 (d, 10.8)	136.4	6.86 (d, 10.8)	136.4	6.86 (d, 10.8)	136.4	6.87 (d, 10.8)	136.9	6.47 (t, 7.2)
25	130.6	–	128.6	–	128.6	–	128.6	–	132.2	–
26	57.4	4.43 (d, 12.8) 4.47 (d, 12.8)	13.0	1.95 (s)	13.0	1.95 (s)	13.0	1.95 (s)	13.1	1.86 (s)
27	171.1	–	172.7	–	172.7	–	172.7	–	172.7	–
28	26.3	1.07 (s)	26.2	1.05 (s)	26.6	1.09 (s)	26.6	1.12 (s)	26.2	1.05 (s)
29	15.4	0.88 (s)	16.0	0.91 (s)	16.0	0.91 (s)	16.9	0.96 (s)	16.0	0.90 (s)
30	19.9	0.93 (s)	19.9	0.93 (s)	19.9	0.93 (s)	20.0	0.94 (s)	19.9	0.91 (s)
Hil										
1	176.8	–	176.9	–	176.9	–	176.8	–	177.1	–
2	56.1	5.02 (d, 7.2)	56.0	5.03 (d, 7.2)	56.0	5.03 (d, 7.2)	56.0	5.04 (d, 7.2)	53.8	4.55 (d, 9.6)
3	39.4	2.83 (m)	39.4	2.77 (m)	39.4	2.77 (m)	39.3	2.77 (m)	41.6	2.36 (m)
4	78.8	4.74 (m)	78.7	4.72 (m)	78.7	4.71 (m)	78.7	4.72 (m)	84.5	4.40 (m)
3-Me	7.9	0.81 (d, 7.6)	8.1	0.81 (d, 7.6)	8.1	0.85 (d, 7.6)	8.1	0.81 (d, 7.6)	12.4	0.93 (d, 7.2)
4-Me	15.7	1.34 (d, 6.4)	15.7	1.33 (d, 6.4)	15.7	1.34 (d, 6.4)	15.7	1.33 (d, 6.4)	19.9	1.40 (d, 6.0)
	Glc I		*Glc I*		*Glc I*		*Glc I*		*Glc I*	
1	105.3	4.41 (d, 8.0)	106.0	4.37 (d, 8.0)	106.2	4.34 (d, 8.0)	105.3	4.38 (d, 8.0)	106.0	4.36 (d, 8.0)
2	78.5	3.71 (m)	79.4	3.90 (m)	77.7	4.02 (m)	78.0	4.06 (m)	79.4	3.89 (m)
3	77.6	3.72 (m)	78.7	3.52 (m)	77.8	3.65 (m)	77.6	3.70 (m)	78.7	3.52 (m)
4	79.7	3.47 (m)	71.1	3.42 (m)	80.1	3.60 (m)	79.4	3.65 (m)	71.1	3.42 (m)
5	76.4	3.32 (m)	78.0	3.61 (m)	76.4	3.28 (m)	76.7	3.41 (m)	78.0	3.61 (m)
6	62.0	3.65 (m) 3.79 (br d, 11.2)	69.9	3.78 (dd, 5.2, 11.2) 4.07 (br d, 11.2)	62.2	3.68 (m)/3.78 (m)	62.6	3.68 (m)/3.80 (m)	69.9	3.78* 4.06 (br d, 11.2)
	Glc II		*Glc II*		*Glc II*		*Glc II*		*Glc II*	
1	102.0	4.90 (d, 7.6)	103.7	4.65 (d, 7.6)	101.9	4.80 (d, 8.0)	102.2	4.91 (d, 7.6)	103.7	4.65 (d, 7.6)
2	78.9	3.39 (m)	76.0	3.23 (m)	79.2	3.42 (m)	79.2	3.43 (m)	76.0	3.23 (m)
3	79.2	3.47 (m)	78.3	3.33 (m)	79.4	3.41 (m)	79.4	3.41 (m)	78.3	3.34 (m)
4	72.6	3.05 (t, 9.2)	71.8	3.20 (m)	72.0	3.08 (m)	72.6	3.11 (m)	71.8	3.20 (m)
5	78.0	3.24 (m)	78.4	3.28 (m)	77.5	3.50 (m)	77.6	3.50 (m)	78.4	3.27 (m)
6	63.7	3.52 (dd, 4.0, 11.2) 3.83 (br d, 11.2)	62.4	3.69 (m)/3.80 (m)	69.9	3.70 (m)/4.05 (m)	70.1	3.70 (m)/4.07 (m)	62.4	3.69 (m)/3.80 (m)
	Rha I		*Glc III*		*Rha I*		*Rha I*		*Glc III*	
1	101.7	5.23 (br s)	102.6	5.03 (d, 7.2)	101.9	5.20 (br s)	101.9	5.20 (br s)	102.6	5.03 (d, 7.2)
2	72.0	3.90 (br s)	83.2	3.39 (m)	72.3	3.89 (br s)	72.1	3.90 (br s)	83.2	3.39 (m)
3	72.2	3.73 (m)	77.5	3.22 (m)	72.2	3.72 (m)	72.2	3.72 (m)	77.6	3.22 (m)
4	74.1	3.39 (m)	71.4	3.34 (m)	74.2	3.38 (m)	74.1	3.38 (m)	71.4	3.33 (m)
5	69.4	4.11 (m)	77.4	3.46 (m)	69.5	4.13 (m)	69.5	4.11 (m)	77.5	3.46 (m)
6	18.4	1.23 (d, 6.4)	62.6	3.69 (m)/3.80 (m)	18.4	1.23 (d, 6.4)	18.4	1.22 (d, 6.4)	62.6	3.69*/3.80*
	Rha II		*Glc IV*		*Rha II*		*Rha II*		*Glc IV*	
1	102.7	4.84 (br s)	105.6	4.59 (d, 7.2)	102.9	4.88 (br s)	102.8	4.87 (br s)	105.6	4.59 (d, 7.2)
2	72.3	3.83 (br s)	76.1	3.34 (m)	72.5	3.83 (br s)	72.4	3.83 (br s)	76.0	3.32 (m)
3	72.0	3.64 (m)	77.1	3.45 (m)	72.2	3.62 (m)	72.1	3.64 (m)	77.1	3.46 (m)
4	73.7	3.39 (m)	71.3	3.29 (m)	73.9	3.38 (m)	73.7	3.38 (m)	71.4	3.29 (m)

(*continued on next page*)

Table 1 (*continued*)

C	1		2		3		4		5	
	δ_C	δ_H (mult, *J* in Hz)	δ_C	δ_H (mult, *J* in Hz)	δ_C	δ_H (mult, *J* in Hz)	δ_C	δ_H (mult, *J* in Hz)	δ_C	δ_H (mult, *J* in Hz)
5	70.6	3.97 (m)	77.7	3.28 (m)	70.8	3.94 (m)	70.6	3.96 (m)	77.8	3.28 (m)
6	18.1	1.27 (d, 6.4)	62.7	3.69 (m)/3.80 (m)	18.3	1.30 (d, 6.4)	18.1	1.28 (d, 6.4)	62.7	3.69 (m)/3.80 (m)
					Glc III		*Glc III*			
1					102.7	5.09 (d, 7.6)	104.6	4.70 (d, 8.0)		
2					83.6	3.32 (m)	75.2	3.17 (m)		
3					78.1	3.34 (m)	77.6	3.70 (m)		
4					71.4	3.34 (m)	71.6	3.30 (m)		
5					77.7	3.65 (m)	77.8	3.33 (m)		
6					62.4	3.68*/3.78*	62.7	3.52 (m)/3.83 (m)		
					Xyl					
1					106.5	4.52 (d, 7.2)				
2					75.7	3.38 (m)				
3					77.4	3.30 (m)				
4					71.0	3.55 (m)				
5					67.2	3.19 (m)/3.94 (m)				

Assignments were done by HSQC, HMBC, and COSY experiments; *overlapped signal; Glc, glucopyranosyl; Rha, rhamnopyranosyl; Xyl, xylopyranosyl; Hil, 4-hydroxyisoleucine lactone.

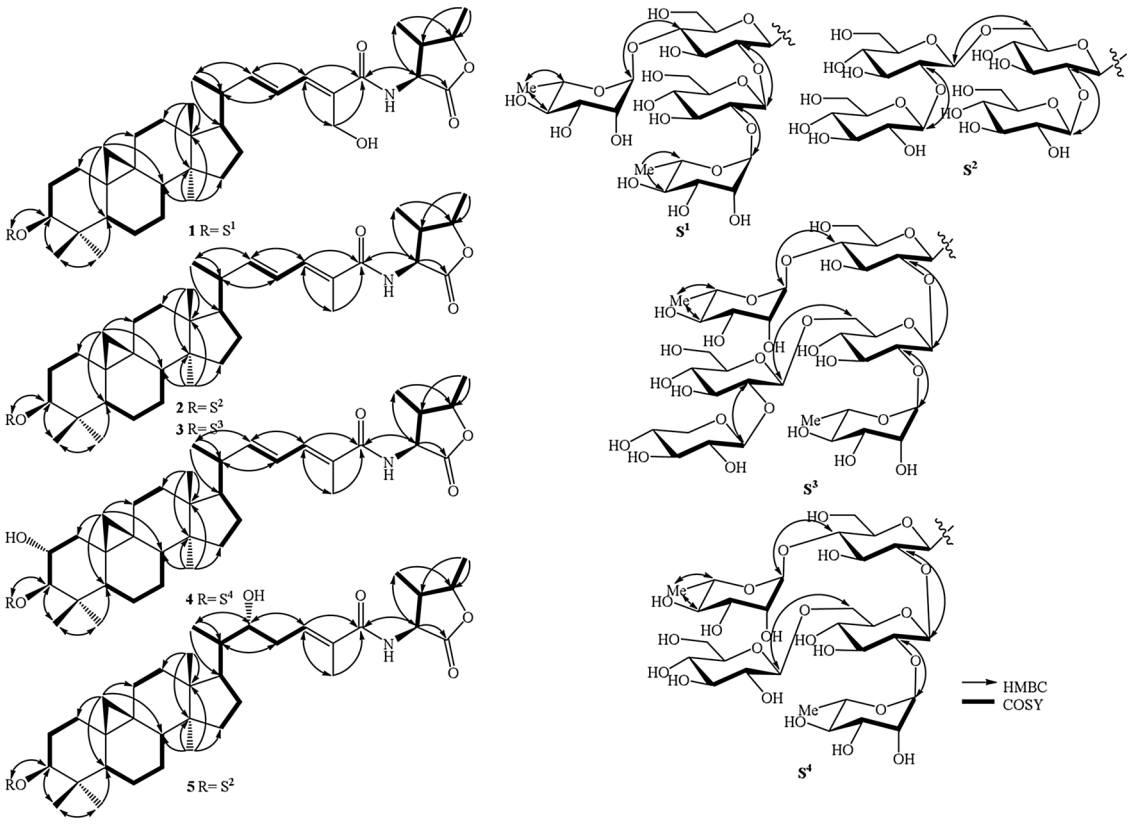

Fig. 2. The key HMBC and COSY correlations of compounds **1–5**.

and glc I C-2 (δ_C 77.7) indicated the sequence of sugar linkages to be *β*-D-xylopyranosyl-(1→2)-*O*-*β*-D-glucopyranosyl-(1→6)-*O*-[*α*-L-rhamnopyranosyl-(1→2)]-*O*-*β*-D-glucopyranosyl-(1→2)-*O*-[*α*-L-rhamnopyranosyl-(1→4)]-*O*-*β*-D-glucopyranoside. The positions of the sugar linkages at C-3 was confirmed by the HMBC correlations from glc I H-1 (δ_H 4.34) to C-3 (δ_C 92.2). Based on the above evidence, the structure of **3** was elucidated as heinsiagenin A 3-*O*-*β*-D-xylopyranosyl-(1→2)-*O*-*β*-D-glucopyranosyl-(1→6)-*O*-[*α*-L-rhamnopyranosyl-(1→2)]-*O*-*β*-D-glucopyranosyl-(1→2)-*O*-[*α*-L-rhamnopyranosyl-(1→4)]-*O*-*β*-D-glucopyranoside and named as mussaglaoside C.

The molecular formula of **4** was determined as $C_{66}H_{105}O_{28}N$ by the HR-ESI-MS at m/z 1382.6703 $[M + Na]^+$ (Calcd. for $[C_{66}H_{105}O_{28}NNa]^+$, 1382.6715). The NMR data of **4** were similar to those of mussaendoside P (Zhao et al., 1994) except for the addition of one sugar unit at Glc II C-6. The HMBC correlations between H_3-28 (δ_H 1.12)/H_3-29 (δ_H 0.96) and C-3 (δ_C 96.8)/C-4 (δ_C 43.2)/C-5 (δ_C 48.7) as well as COSY correlations between H-2 (δ_H 3.75) and H-3 (δ_H 2.97) indicated the position of a hydroxyl group at C-2 and an oxygenated group at C-3. The large coupling constant of H-2 and H-3, J = 8.8 Hz and the NOESY correlations between H-2 (δ_H 3.75) and H_3-29 (δ_H 0.96)/H_a-19 (δ_H 0.47) indicated that the orientations of H-2 and H-3 were *axial*. The HMBC correlations from H_3-21 (δ_H 1.04) to C-17 (δ_C 53.1)/C-20 (δ_C 42.2)/C-22 (δ_C 149.6), H-24 (δ_H 6.87) to C-22/C-23 (δ_C 124.6)/C-25 (δ_C 128.6)/C-26 (δ_C 13.0)/C-27 (δ_C 172.7), from H-22 (δ_H

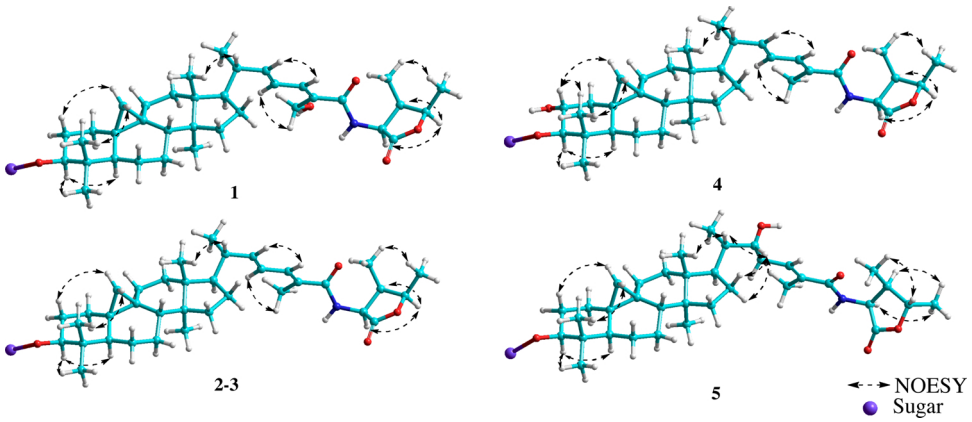

Fig. 3. The key NOESY correlations of compounds **1–5**.

5.93) to C-17/ C-20/C-21 (δ_C 20.2)/C-24 (δ_C 136.4) confirmed the positions of two double bonds at C-22/C-23 and C-24/C-25. In addition, the large coupling constant of H-22 and H-23, J = 14.8 Hz and the NOESY correlations between H-23 (δ_H 6.34) and H_3-26 (δ_H 1.95) confirmed the configurations of both double bonds as *E*. Acid hydrolysis of **4** gave L-rhamnose and D-glucose (identified as TMS derivatives by GC–MS) GC–MS). The HMBC correlations between rha II H-1 (δ_H 4.87) to glc I C-4 (δ_C 79.4), rha I H-1 (δ_H 5.20) and glc II C-2 (δ_C 79.2), glc III H-1 (δ_H 4.70) and glc II C-6 (δ_C 70.1), glc II H-1 (δ_H 4.91) and glc I C-2 (δ_C 78.0), and between glc I H-1 (δ_H 4.38) and C-3 (δ_C 96.8) indicated the sequence of sugar moieties. Thus, the structure of **4** was determined as 2*α*-hydroxyheinsiagenin A 3-*O*-*β*-D-glucopyranosyl-(1→6)-*O*-[*α*-L-rhamnopyranosyl-(1→2)]-*O*-*β*-D-glucopyranosyl-(1→2)-*O*-[*α*-L-rhamnopyranosyl-(1→4)]-*O*-*β*-D-glucopyranoside and named as mussaglaoside D.

The HR-ESI-MS of **5** corresponded to the molecular formula of $C_{60}H_{97}O_{25}N$. The ^{1}H and ^{13}C-NMR spectral data of **5** were similar to those of **2** except for the difference branch chain of cycloartane. In addition, the position of a hydroxyl group at C-22 was proved by HMBC correlations between H_3-21 (δ_H 0.93) and C-17 (δ_C 50.5)/C-20 (δ_C 43.9)/C-22 (δ_C 74.2). The *α*-configuration of the hydroxyl group at C-22 was proven by NOESY correlations between H-22 (δ_H 3.77) and H-20 (δ_H 1.73)/H-16 (δ_H 1.37 and 1.83). The 4-hydroxyisoleucine γ-lactone connected with cycloartane aglycone *via* the *N*-amide bond which was confirmed by HMBC correlations from hil H-2 (δ_H 4.55) to C-27 (δ_C 172.7). The ^{13}C-NMR chemical shift of hil 3-Me (δ_C 12.4) and hil 4-Me (δ_C 19.9) confirmed the configuration of 4-hydroxyisoleucine γ-lactone (2*S**,3*R**,4*S**) by comparison with those of mussaglaosides B–D (**2–4**) [hil 3-Me (δ_C 8.1) and hil 4-Me (δ_C 15.7)] and (2*S*,3*R*,4*S*)-4-hydroxyisoleucine γ-lactone hydrochloride [3-Me (δ_C 13.0) and 4-Me (δ_C 19.5)] (Wang et al., 2002), and were further confirmed by NOESY correlations between hil 4-Me (δ_H 1.40) and hil H-2 (δ_H 4.55)/hil H-3 (δ_H 2.36). The sugar linkages of **5** were proven to be similar to those of mussaglaoside B (**2**). Thus, compound **5** was determined as *N*-(2*S**,3*R**,4*S**)-hydroxyisoleucine γ-lactone-22-hydroxycycloart-24(25)-ene-27-amide 3-*O*-*β*-D-glucopyranosyl-(1→2)-*O*-*β*-D-glucopyranosyl-(1→6)-*O*-[*β*-D-glucopyranosyl-(1→2)]-*O*-*β*-D-glucopyranoside and named mussaglaoside E.

The known compounds (**6–10**) were characterized as mussaendoside O (Zhao et al., 1994), mussaendoside G (Weimin et al., 1996) mussaendoside U (Zhao et al., 1997), mussaendoside P (Zhao et al., 1994), and mussaendoside Q (Zhao et al., 1994), respectively by analysis of NMR spectroscopic data and in comparison in the literature.

To determine the inhibitory effect of ANO1 channel activity on HT29 human colon cancer cell lines, yellow fluorescent protein (YFP) reduction assays were performed using triterpenoid saponins (**1–10**) isolated from *M. glabra*. ANO1 chloride channel activity was measured using HT29 (human colon cancer cells) endogeneously expressing human ANO1 and the genetically encoded iodide-sensing fluorescent protein, YFP-F46 L/H148Q/I152 L (Seo et al., 2016). HT-29 cells were pre-incubated with test compounds in PBS prior to the addition of a solution containing iodide and ATP. In the presence of an ANO1 inhibitor, YFP fluorescence quenching by iodide intake through ANO1 was inhibited. As shown in Table 2, compounds **2–6**, and **10** blocked iodide influx by > 25% at the concentration of 30 μM. Compound **6** significantly inhibited ANO1 chloride channel activity by 53% without any cytotoxicity. Compound **6** was further evaluated at various concentrations to get IC_{50} value. As the results, compounds **6** strongly inhibited chloride channel activity with an IC_{50} value of 22.0 ± 1.7 μM. These data suggest that triterpenes from the leaves of *M. glabra* may be powerful candidates in the development of novel therapeutic antitumor and inhibitory agents for excessive smooth muscle contraction and diarrhea symptoms *via* ANO1 inhibition.

3. Experimental

3.1. General

All NMR spectra were recorded on an AGILENT 400 MHz. Data processing was carried out with the MestReNova ver. 9.0.1. Optical rotations were determined on a Jasco DIP-370 digital polarimeter. HR-ESI-MS spectra were obtained using AGILENT 6550 iFunnel Q-TOF LC/MS system. HPLC was carried out using an AGILENT 1200 HPLC system. Column chromatography (CC) was performed on silica-gel (Kieselgel 60, 230–400 mesh, Merck) or RP-18 resins (30–50 μm, Fuji Silysia Chemical Ltd.). For thin layer chromatography (TLC), pre-coated silica-gel 60 F_{254} (0.25 mm, Merck) and RP-18 $F_{254}S$ (0.25 mm, Merck) plates were used.

Table 2
PAR2 receptor inhibition of compounds **1-10** at 30 μM in HT29-YFP cells.

Compounds	PAR2 receptor inhibition (%)
1	< 25
2	30.8 ± 1.5
3	42.7 ± 3.1
4	33.0 ± 2.7
5	34.8 ± 4.5
6	53.4 ± 3.4
7	< 25
8	< 25
9	37.2 ± 2.5
10	< 25

3.2. Plant material

The aerial parts of *Mussaenda glabra* Vahl were collected at Me Linh, Vinh Phuc, Vietnam in February 2017 and identified by Dr. Nguyen The Cuong, Institute of Ecology and Biological Resources, VAST. A voucher specimen (NCCT-P67) was deposited at the Institute of Marine Biochemistry, VAST.

3.3. Extraction and isolation

The dried powder of aerial parts of *M. glabra* (5.2 kg) was sonicated 3 times with hot methanol and then filtered through filter paper, removed solvent to yield 270 g of a dark solid extract. The extract was suspended in water and successively partitioned with *n*-hexane, dichloromethane, and ethyl acetate solvents giving *n*-hexane (MG1, 45 g), dichloromethane (MG2, 90 g), ethyl acetate extracts (MG3, 23 g) and water layer (MG4). Continuously, the water layer was chromatographed on a Diaion HP-20 column eluting with water to remove sugar components, then increase concentration of methanol in water (50 and 100%, v/v) to obtain two fractions, MG4A and MG4B, respectively. The MG4A fraction was chromatographed on a silica gel column eluting with dichloromethane/methanol (20/1, 10/1, 5/1, 2.5/1, v/v) to give four su**b**-fractions MG4A1-MG4A4. MG4A3 was chromatographed on a RP-18 column eluting with acetone/water (1/1.2, v/v) to give four smaller fractions, MG4A3A-MG4A3D. MG4A3C fraction was chromatographed on a silica gel column eluting with dichloromethane/methanol/water (3/1/0.1, v/v/v) to give two fractions, MG4A3C1-MG4A3C2. MG4A3C1 further chromatographed on HPLC using J'sphere ODS M-80, 150 mm × 20 mm column, ACN in H_2O (38%, v/v) and a flow rate of 3 mL/min to yield compounds **4** (8.0 mg) and **10** (40.0 mg). Compound **5** (6.0 mg) was obtained from MG4A3C2 chromatographed on HPLC using J'sphere ODS M-80, 150 mm × 20 mm column, ACN in H_2O (35%, v/v), and a flow rate of 3 mL/min. The MG4B fraction was separated into four smaller fraction MG4B1-MG4B4 by silica gel column and gradient solvent system of dichloromethane/methanol (20/1, 10/1, 5/1, 2.5/1, v/v). MG4B2 was chromatographed on a RP-18 column eluting with acetone/water (1/1, v/v) to give three smaller fractions, MG4B2A-MG4B2C. MG4B2A fraction was chromatographed on a silica gel column eluting with dichloromethane/acetone/water (1/4/0.3, v/v/v) to give two fractions, MG4B2A1-MG4B2A2. The MG4B2A1 was purified on HPLC column (J'sphere ODS M-80, 150 mm × 20 mm column) eluting with 45% acetonitrile to yield **1** (20.0 mg). MG4B2A2 chromatographed on HPLC using J'sphere ODS M-80, 150 mm × 20 mm column, 45% CAN in H_2O to yield **2** (6.0 mg). MG4B2C fraction was chromatographed on a silica gel column eluting with dichloromethane/methanol/water (3/1/0.1, v/v/v) to give two fractions, MG4B2C1 and MG4B2C2. MG4B2C2 was further chromatographed on HPLC using J'sphere ODS M-80, 150 mm × 20 mm column, ACN in H_2O (45%) and a flow rate of 3 mL/min to yield **6** (60.0 mg). MG4B4 was chromatographed on a RP-18 column eluting with acetone/water (1/1.2, v/v) to give five smaller fractions, MG4B4A-MG4B4E. MG4B4A fraction was chromatographed on a silica gel column eluting with dichloromethane/acetone/water (1/4/0.3, v/v/v) to give two fractions, MG4B4A1-MG4B4A2. MG4B4A2 was further chromatographed on HPLC using J'sphere ODS M-80, 150 mm × 20 mm column, ACN in H_2O (45%) to yield **9** (30.0 mg). MG4B4C fraction was chromatographed on a silica gel column eluting with dichloromethane/methanol/water (3/1/0.1, v/v/v) to give two fractions, MG4B4C1-MG4B4C2. The MG4B4C1 was purified on HPLC column (J'sphere, ODS M-80, 150 mm × 20 mm) eluting with 40% acetonitrile to yield compounds **8** (40.0 mg) and **7** (7.0 mg). Finally, compound **3** (15.0 mg) was isolated from the MG4B4C2 chromatographed on HPLC using J'sphere ODS M-80, 150 mm × 20 mm column, AC**N**-H_2O (40–60, v/v).

3.3.1. Mussaglaoside A (1)

White amorphous powder. $[\alpha]_D^{25}$ = +30.0 (*c* 1.0 MeOH). HR-ESI-MS m/z: 1220.6189 $[M + Na]^+$ (Calcd. for $[C_{60}H_{95}O_{23}NNa]^+$, 1220.6187). ^{1}H- and ^{13}C-NMR (CD_3OD): see Table 1.

3.3.2. Mussaglaoside B (2)

White amorphous powder. $[\alpha]_D^{25}$ = +45.0 (*c* 1.0 MeOH). HR-ESI-MS m/z: 1236.6134 $[M + Na]^+$ (Calcd. for $[C_{60}H_{95}O_{24}NNa]^+$, 1236.6136). ^{1}H- and ^{13}C-NMR (CD_3OD): see Table 1.

3.3.3. Mussaglaoside C (3)

White amorphous powder. $[\alpha]_D^{25}$ = +39.0 (*c* 1.0 MeOH). HR-ESI-MS m/z: 1498.7178 $[M + Na]^+$ (Calcd. for $[C_{71}H_{113}O_{31}NNa]^+$, 1498.7189). ^{1}H- and ^{13}C-NMR (CD_3OD): see Table 1.

3.3.4. Mussaglaoside D (4)

White amorphous powder. $[\alpha]_D^{25}$ = +52.0 (*c* 1.0 MeOH). HR-ESI-MS m/z: 1382.6703 $[M + Na]^+$ (Calcd. for $[C_{66}H_{105}O_{28}NNa]^+$, 1382.6715). ^{1}H- and ^{13}C-NMR (CD_3OD): see Table 1.

3.3.5. Mussaglaoside E (5)

White amorphous powder. $[\alpha]_D^{25}$ = +21.0 (*c* 1.0 MeOH). HR-ESI-MS m/z: 1254.6248 $[M + Na]^+$ (Calcd. for $[C_{60}H_{97}O_{25}NNa]^+$, 1254.6242). ^{1}H- and ^{13}C-NMR (CD_3OD): see Table 1.

3.4. Acid hydrolysis

Each compound (**1**–**5**, 2.0 mg) was separately dissolved in 1.0 N HCl (dioxane—H_2O, 1:1, v/v, 1.0 mL) and heated to 80 °C in a water bath for 3 h. Acidic solution was neutralized with Ag_2CO_3 with the solvent thoroughly removed under a N_2 stream overnight. After extraction with $CHCl_3$, the aqueous layer was concentrated to dryness using N_2. The residue was dissolved in dry pyridine (0.1 mL), followed by addition of L-cysteine methyl ester hydrochloride in pyridine (0.06 M, 0.1 mL). The reaction mixture was heated at 60 °C for 2 h. Trimethylsilylimidazole solution (0.1 mL) was then added, followed by heating at 60 °C for 1.5 h. The dried product was partitioned with *n*-hexane and H_2O (0.1 mL each), and the organic layer was analyzed by gas chromatography (GC): column DB-5 (0.32 mm ID × 30 m length), detector FID, column temp 210 °C, injector temp 270 °C, detector temp 300 °C, carrier gas He (2 mL/min). Under these conditions, the standard sugars gave peaks at t_R (min) 14.11 and 14.26 for D- and L-glucose, 8.21 and 8.66 for D- and L-xylose, and 4.50 for L-rhamnose, respectively. Peaks at t_R (min) 14.11 and 4.50 of D-glucose and L-rhamnose for **1** and **4**; 14.11 of D-glucose for **2** and **5**; 14.11, 8.21, and 4.50 of D-glucose, D-xylose, and L-rhamnose for **3** were observed.

3.5. Yellow fluorescent protein (YFP) fluorescence measurement

Calcium-activated chloride channel (ANO1) and YFP expressing HT29 cells were plated in 96-well black-walled microplates (Corning Inc., Corning, NY) at a density of 15,000 cells per well. YFP reduction analysis was perforemed usnig FLUOstar Omega microplate reader (BMG Labtech, Ortenberg, Germany) and MARS Data Analysis Software (BMG Labtech) as described in previous study (Seo et al., 2016). Briefly, each well of 96-well plate was washed 2 times in PBS (200 μL/wash) and test compounds were added to each well at 30 μM final concentration. After incubation at 37 ℃ for 10 min, 96-well plates were transferred to a plate reader for fluorescence analysis. Each well was individually assayed for ANO1-mediated I^- influx by monitoring YFP fluorescence continuously (400 ms per point) for 2 s (baseline), then 140 mM I^- solution containing 200 μM ATP was added at 2 s and then YFP fluorescence was recorded for 6 s. The initial iodide influx rate was determined from the initial slope of fluorescence reduction by nonlinear regression after iodide injection with ATP.

Acknowledgment

This research is funded by Vietnam National Foundation for Science and Technology Development (NAFOSTED) under grant number 104.01-2016.27, Vietnam and by the National Research Foundation of Korea (NRF) grant [NRF-2016R1A2B4006742] funded by the Ministry of Education, Science and Technology, Republic of Korea.

Appendix A. Supplementary data

Supplementary material related to this article can be found, in the online version, at doi:https://doi.org/10.1016/j.phytol.2019.07.006.

References

Astalakshmi, N., Sundara, G.R., 2017. A comprehensive review on the genus: Mussaenda. Int. J. Pharm. Sci. Res. 8, 534–541.

Bill, A., Hall, M.L., Borawski, J., Hodgson, C., Jenkins, J., Piechon, P., Popa, O., Rothwell, C., Tranter, P., Tria, S., 2014. Small molecule-facilitated degradation of ANO1 protein: a new targeting approach for anticancer therapeutics. J. Biol. Chem. 289, 11029–11041.

Chi, V.V., 1999. The Dictionary of Vietnamese Medicinal Plants. Hanoi Medicine, Hanoi, Vietnam.

De, U.C., Ghosh, R., Chowdhury, S., Dinda, B., 2012. New iridoid from aerial parts of Mussaenda roxburghii. Nat. Prod. Comm. 7, 1–2.

Dinda, B., Majumder, S., Arima, S., Sato, N., Harigaya, Y., 2008. Iridoid glucoside and sterol galactoside from Mussaenda macrophylla. J. Nat. Med. 62, 447–451.

Harvey, A.L., Edrada-Ebel, R., Quinn, R.J., 2015. The re-emergence of natural products for drug discovery in the genomics era. Nat. Rev. Drug Discov. 14, 111.

Hwang, S.J., Basma, N., Sanders, K.M., Ward, S.M., 2016. Effects of new-generation inhibitors of the calcium-activated chloride channel anoctamin 1 on slow waves in the gastrointestinal tract. Br. J. Pharmacol. 173, 1339–1349.

Mohamed, S.M., Backheet, E.Y., Bayoumi, S.A., Ross, S.A., 2016. New cycloartane saponin and monoterpenoid glucoindole alkaloids from Mussaenda luteola. Fitoterapia 110, 129–134.

Namkung, W., Thiagarajah, J.R., Phuan, P.-W., Verkman, A., 2010. Inhibition of Ca2+-activated Cl− channels by gallotannins as a possible molecular basis for health benefits of red wine and green tea. Faseb J. 24, 4178–4186.

Seo, Y., Lee, H.K., Park, J., Jeon, D.-k., Jo, S., Jo, M., Namkung, W., 2016. Ani9, a novel potent small-molecule ANO1 inhibitor with negligible effect on ANO2. PLoS One 11, e0155771.

Wang, Q., Ouazzani, J., Sasaki, N.A., Potier, P., 2002. A practical synthesis of (2S,3R,4S)-4-hydroxyisoleucine, a potent insulinotropic α-amino acid from fenugreek. Eur. J. Org. Chem. 2002, 834–839.

Weimin, Z., Rensheng, X., Guowei, Q., Vaisar, T., Lee, M.S., 1996. Saponins from Mussaenda pubescens. Phytochemistry 42, 1131–1134.

Zhang, X., Li, H., Zhang, H., Liu, Y., Huo, L., Jia, Z., Xue, Y., Sun, X., Zhang, W., 2017. Inhibition of transmembrane member 16A calcium-activated chloride channels by natural flavonoids contributes to flavonoid anticancer effects. Br. J. Pharmacol. 174, 2334–2345.

Zhao, W., Xu, J., Qin, G., Xu, R., Wu, H., Weng, G., 1994. New triterpenoid saponins from Mussaenda pubescens. J. Nat. Prod. 57, 1613–1618.

Zhao, W., Wolfender, J.-L., Hostettmann, K., Cheng, K., Xu, R., Qin, G., 1997. Triterpenes and triterpenoid saponins from Mussaenda pubescens. Phytochemistry 45, 1073–1078.